

## CCDC86 promotes the aggressive behavior of nasopharyngeal carcinoma by positively regulating EGFR and activating the PI3K/Akt signaling

Zhi WANG<sup>1\*</sup>, Tao ZHOU<sup>2\*</sup>, Xubo CHEN<sup>1</sup>, Xinhua ZHU<sup>1</sup>, Bing LIAO<sup>1</sup>, Jianguo LIU<sup>1</sup>, Siqi LI<sup>1</sup>, Ting TAN<sup>1</sup>, Yuehui LIU<sup>1\*</sup>

<sup>1</sup>Department of Otorhinolaryngology Head and Neck Surgery, The Second Affiliated Hospital of Nanchang University, Nanchang, China;

<sup>2</sup>Department of Thyroid Surgery, The Second Affiliated Hospital of Nanchang University, Nanchang, China

\*Correspondence: liuyuehui2021@126.com

\*Contributed equally to the work.

Received October 21, 2022 / Accepted November 24, 2023

Nasopharyngeal carcinoma (NPC) is a common malignant tumor of the head and neck. A number of studies have confirmed that coiled-coil domain-containing protein 86 (CCDC86) plays an important role in the pathogenesis of lymphoma but the role of CCDC86 in NPC has not yet been reported. Here, *in vivo* and *in vitro* experiments were conducted to explore whether CCDC86 plays a role in the pathogenesis of NPC and to identify the specific mechanism. We found that CCDC86 was highly expressed in NPC tissues and cells, and the expression level of CCDC86 was correlated with the prognosis of patients with advanced NPC. CCDC86 promoted the proliferation, invasion, and migration of NPC cells *in vivo* and *in vitro* by promoting the EMT process and upregulating the expression of MMPs. Then, we confirmed that EGFR is a downstream target gene of CCDC86 and that CCDC86 can promote the proliferation, invasion, and migration of NPC cells by upregulating the expression of EGFR and activating downstream PI3K/Akt. Furthermore, we confirmed that CCDC86 did not directly bind to EGFR but positively regulated EGFR by binding to NPM1. CCDC86 is expected to be used as a novel biomarker and therapeutic target for predicting the prognosis of NPC.

*Key words: nasopharyngeal carcinoma; CCDC86; invasion and migration; EGFR; PI3K-Akt signaling*

Nasopharyngeal carcinoma (NPC) is a malignant tumor originating from the nasopharynx epithelium. It is estimated that, in 2018, the worldwide incidence of NPC was 130,000 with mortality reaching 73,000 [1]. Although the effect of diagnostic methods, surgical treatment, and chemoradiotherapy in treating NPC has been continuously improved in recent years, weaknesses remain, such as a high recurrence rate, easy metastasis and poor prognosis, which are related to the unclear molecular mechanism of the occurrence and recurrence of NPC. Therefore, enhancing the understanding of the molecular mechanisms underlying NPC is critically important for the exploitation of more efficient treatments for NPC.

The coiled-coil domain-containing protein 86 (CCDC86) gene is initially induced in hematopoietic stem cells by interleukin-3, encoding a phosphorylated nuclear protein composed of an N-terminal repeating sequence and C-terminal coiled-coil sequence. CCDC86 mRNA is mainly expressed in the heart, liver, and intestine; it is activated in peripheral CD4<sup>+</sup> T cells and CD8<sup>+</sup> T cells; and CCDC86 mRNA is mainly expressed in the nucleus in the BA/F3 cell

line [2]. Some studies have reported that CCDC86 is associated with the occurrence of lymphoma. In mice, CCDC86 knockdown inhibited myc gene expression in invasive tumor cells and regulated the gene expression associated with lymphoma, revealing that CCDC86 is closely related to the occurrence of lymphoma [3]. However, there have been no reports on the effect of CCDC86 on NPC.

Epidermal growth factor receptor (EGFR) is a member of the ErbB family and is widely distributed on the surfaces of mammalian epithelial cells, fibroblasts, glial cells, keratinocytes, and other cells and plays important regulatory roles in cellular physiological processes. Activation of EGFR by ligands such as EGF can lead to increased EGFR phosphorylation, further activating downstream signal transduction pathways, and enabling its participation in various physiological processes, such as cell growth and proliferation [4]. It has been confirmed that the expression and function of EGFR are abnormal in a variety of human malignant tumor tissues and tumor cell lines [5–10], including bladder cancer, ovarian cancer, NPC, breast cancer, glioma, pancreatic cancer, prostate cancer, and esophageal cancer. Previous

studies have shown that EGFR expression was significantly higher in NPC tissues than in normal nasopharyngeal tissues [11], and inhibiting the expression of EGFR could reduce the invasion and metastatic abilities of NPC cell lines [12].

The PI3K/Akt signaling pathway is a downstream pathway of EGFR and is dysregulated in most malignant tumors. The abnormally activated PI3K/Akt pathway plays an important role in the infinite proliferation, angiogenesis, and tumor metastasis of cancer cells. EGFR mainly stimulates Ras proteins, inducing a phosphorylation cascade that activates the PI3K/Akt signaling pathway to promote the proliferation of tumor cells, inhibit cell apoptosis, and enhance tumor cell invasion and migration, and tolerance to treatment [13]. Some scholars have called the EGFR-PI3K/Akt signaling pathway one of the most classic tumorigenic pathways. Considering previous studies, we speculated that CCDC86 can promote the proliferation, apoptosis, invasion, and migration of NPC by activating the EGFR-PI3K/Akt signaling pathway.

In this study, we aimed to investigate the role of CCDC86 in NPC and the associations between CCDC86 and EGFR. Then, we sought to determine whether CCDC86 affects NPC cells by regulating the EGFR-PI3K/Akt signaling pathway and the specific mechanism of this action. Our results will provide new ideas for the targeted treatment of NPC.

## Patients and methods

**Patients and clinical samples.** Immunohistochemical staining was performed on 124 NPC samples embedded in paraffin sections and 50 normal nasopharyngeal epithelium (NNE) samples embedded in paraffin sections obtained from the Second Affiliated Hospital of Nanchang University, and the associated clinical data were analyzed retrospectively. No patients received anticancer treatments before enrolling in this study. The tumor grades of all the samples were assessed in accordance with World Health Organization (WHO) criteria. The median follow-up time for these 124 NPC patients was 72 months. The Ethics Committee of the Second Affiliated Hospital of Nanchang University approved the use of these tissues in this study (approval No. 202210311014). Written informed consent was obtained from all patients and healthy participants. All methods were performed in accordance with the relevant guidelines and regulations.

**Immunohistochemical staining.** Tissue sections were repaired with 0.01 M sodium citrate buffer and incubated for 1 h with 3% hydrogen peroxide to eliminate endogenous peroxidase activity after deparaffinization and rehydration. After antigen retrieval, sections were incubated with CCDC86 antibody (1:1000) at 4 °C overnight, then with the secondary antibody for 1 h at room temperature. Subsequently, 3,3'-diaminobenzidine (DAB) reagent (ZSGB-BIO, Beijing) was used for the peroxidase reaction and hematoxylin was used for counterstaining. Images were acquired under a microscope (Olympus C-5050, Japan). The immunohistochemistry results were independently evalu-

ated by two pathologists who were blinded to sample status. The intensity of CCDC86 staining was scored and graded as follows: staining intensity score, 0 point (negative), 1 point (I), 2 points (II), 3 points (III); Positive staining score: 0 point (negative), 1 point (1–25%), 2 points (26–50%), 3 points (51–75%), 4 points (76–100%). Total score and grouping: CCDC86 protein expression: the product of “staining intensity score” and “staining positive rate score” was used. According to the above products,  $\leq 6$  was divided into the CCDC86 low-expression group,  $> 6$  was divided into the high-expression group.

**Cell lines and cell culture.** NPC-derived cell lines (HONE1, HK1, CNE1, CNE2, CNE2Z, 5-8F, and 6-10 B cells) were cultured in Roswell Park Memorial Institute-1640 (RPMI-1640) medium (Thermo Fisher Scientific, Waltham, MA, USA) supplemented with 10% fetal bovine serum (FBS; Invitrogen, Carlsbad, CA, USA). The human immortalized nasopharyngeal epithelial cell lines NP69 and NP460 were incubated in keratinocyte serum-free medium (Invitrogen, Carlsbad, CA, USA). All these cells were cultured in a 37 °C humidified incubator containing 5% CO<sub>2</sub>. All cell lines were purchased from the Shanghai Institute of Biological Sciences Cell Resource Center of the Chinese Academy of Sciences (Shanghai, China).

**RNA extraction and quantitative real time-polymerase chain reaction (qRT-PCR).** Total RNA was extracted using TRIzol reagent (Invitrogen, Carlsbad, CA, USA) based on the manufacturer's protocol. Extracted RNA was reverse transcribed into complementary DNA (cDNA) using a cDNA synthesis kit (TransGen Biotech, Beijing, China). qRT-PCR was conducted on an ABI 7500 instrument (Applied Biosystems, Foster City, CA, USA) using SYBR Green Mix (TaKaRa, Dalian, Liaoning, China). The following primers were used: CCDC86: (F) 5'-AGCGTCAGCAAGACCTACACC-3', (R) 5'-CCTCCTTATCTGGGCCAACT-3'; EGFR: (F) 5'-CCCACTCATGCTCTACAACCC-3', (R) 5'-TCGCACTTCTTACACTTGCGG-3'; GAPDH: (F) 5'-TGACTTCAACAGCGACACCCA-3', (R) 5'-CACCCCTGTTGCTGTAGCCAAA-3'. The primers were synthesized by BGI (Shenzhen, China). The relative expression levels were detected using the 2<sup>- $\Delta\Delta C_t$</sup>  method using GAPDH as an internal control. Each qRT-PCR was performed in triplicate.

**Western blot (WB) analysis.** Total protein was extracted from the indicated NPC cells using radioimmunoprecipitation assay (RIPA) lysis buffer (Beyotime, Beijing, China) following the manufacturer's protocol. Protein concentration was detected using a bicinchoninic acid (BCA) protein determination kit (Beyotime, Beijing, China). Subsequently, equal amounts of protein were separated using 10% sodium dodecyl sulfate-polyacrylamide gel electrophoresis (SDS-PAGE) and were then transferred to polyvinylidene fluoride (PVDF) membranes (Millipore, Germany). Then, the membrane is trimmed according to the molecular weight of the target protein. The trimmed membranes were incubated with 5% fat-free milk at room temperature for 2 h and then incubated

with different primary antibodies at 4°C overnight. Next, the membranes were washed three times with Tris-buffered saline with Tween-20 and were then incubated with secondary antibodies. The blots were visualized using an enhanced ECL kit (Pierce, Thermo Fisher Scientific, IL, USA). The experiment was performed three separate times. Detailed information on the antibodies for WB used in this study is shown in Supplementary Table S1.

**Vector construction, cell transfection, and stable cell line construction.** Human full-length cDNA of CCDC86 was cloned into the expression plasmid Ubi-MCS-3flag-CBh-gcGFP-IRES-puromycin (GeneChem Shanghai, China), which was then named oe-CCDC86, and an empty lentiviral expression vector was used as a control (oe-NC). Short hairpin RNA (shRNA) sequences were designed by Shanghai GeneChem Co., Ltd. (Shanghai, China) to target human CCDC86. Then, standard shRNA was inserted into a lentiviral hU6-MCS-Ubiquitin-EGFP-IRES-puromycin vector (GeneChem Shanghai, China), named sh-CCDC86, and the negative control was named oe-NC. Stable cell lines were generated using puromycin. The overexpression and knockdown efficiencies were determined by WB analysis.

EGFR agonist (recombinant human EGF) was purchased from PeproTech (USA). Transfection was conducted following the manufacturer's protocol [14]. After 24 h of transfection, the cells were harvested for use in further experiments.

**Microarray screening of CCDC86 downstream target genes.** To screen the downstream target genes of CCDC86 in NPC cells and to further elucidate the correlations between CCDC86 and EGFR, microarray screening analysis and IPA were performed by Shanghai GeneChem Co., Ltd. (Shanghai, China) to analyze the target genes or proteins with which CCDC86 might interact and the potential CCDC86-EGFR co-expression network. The experimental process of gene chip microarray is as follows: After constructing CCDC86 knockdown cells, RNA extraction is performed and Thermo NanoDrop 2000 was used to conduct the quality inspection of RNA samples. RNA samples with a purity between 1.7 and 2.2 are qualified samples. Then the information is collected through IVT, chip hybridization, chip washing and dyeing, chip scanning. Finally, IPA analysis was performed and the gene network interaction map was constructed to find the target genes related to the CCDC86 function.

**Cell proliferation assay.** Cell counting kit-8 (CCK-8) assays and 5-ethynyl-20-deoxyuridine (EdU) incorporation assays were conducted to evaluate cell proliferation. For the CCK-8 assays, the indicated NPC cells were plated in 96-well plates at a density of  $2.5 \times 10^3$  cells/well. Subsequently, 10 ml of CCK-8 solution (Solarbio, Beijing, China) was added to each well and incubated for another 1 h at 37°C. The optical density (OD) at 450 nm was detected to indicate the cell proliferation rate using a microplate reader. EdU incorporation assays were conducted using an EdU Kit (RiboBio, Guangzhou, China) following the manufacturer's protocol.

The results were counted using a Zeiss photomicroscope (Carl Zeiss, Oberkochen, Germany).

**Colony formation assay.** First, 5-8F cells were seeded in 6-well plates at a density of 200, 400, and 800 cells/well to determine the appropriate cell number for the colony formation assay. We chose 400 cells for the following clone formation assay. After incubation for 14 days, the cell colonies were washed with phosphate-buffered solution (PBS; Gibco, Grand Island, NY, USA) and fixed with methanol for 15 min at room temperature. Subsequently, 0.1% crystal violet (Solarbio, Beijing, China) was added to stain the colonies for 15 min at room temperature. Then, a microscope was used to count the fields, each of which contained more than 50 colonies. Finally, the 6-well plate was photographed with a digital camera.

**Cell migration and invasion assays.** Transwell migration and invasion assays were conducted to evaluate cell migration and invasion, respectively. Transwell invasion assays were carried out using a Transwell chamber (Corning, New York, NY, USA) with 8 µm pores coated with Matrigel (BD Biosciences, Franklin Lakes, NJ, USA). Transwell migration assays were carried out using a Transwell chamber (Corning) with 8 µm pores without Matrigel. The indicated NPC cells ( $2 \times 10^4$  cells for the invasion assay and  $1 \times 10^4$  cells for the migration assay) were resuspended in a serum-free medium and plated into the upper chamber. Medium containing 10% FBS was plated into the lower chamber. After incubation for 48 h (for 5-8F cells) or 72 h (for CNE2Z cells), the cells remaining on the upper side were removed. The migrated or invading cells on the lower side of the transwell chamber were fixed in 10% methanol, stained using 0.1% crystal violet for 15 min at room temperature, then counted and imaged (randomly selected 3 areas under the microscope to count the number of cells and calculated the average value) using a Zeiss photomicroscope (magnification,  $\times 100$ ). The assays were conducted three separate times.

**Wound healing assay.** NPC cells were cultured and seeded in 6-well plates at a density of  $1 \times 10^6$  cells per well. After cells reached 90% confluency, a straight line was scraped in the cell monolayer with a 10 µl pipette tip to create a scratch, the cells were washed with PBS twice, and the medium was replaced with a serum-free medium. Images were captured at 0 and 24 h following the scratch was made to evaluate cell migration.

**Mass spectrometry (MS) assay.** MS assays were conducted to identify the possible proteins interacting with the CCDC86 protein in NPC cell lines. CNE2Z cells were harvested 48 h after transfection with sh-CCDC86. An appropriate amount of cell lysis buffer (including protease inhibitor) was added (1 ml/ $1 \times 10^7$  cells), and the cells were cleaved on ice for 10 min. The cells in the lysis buffer were centrifuged at 4°C for 10 min at a maximum rotation speed of  $13,000 \times g$ . Then, a small amount of total protein lysate was harvested as an input sample (the positive control). The remaining lysate was added to the cell lysate in which

5 µg of anti-CCDC86 (Thermo Fisher, A302-481A, USA) or anti-IgG (as the negative control) antibody had been added and then incubated overnight at 4 °C with slow shaking. 20 µl of protein A agarose magnetic beads were washed with an appropriate amount of cleavage buffer 3 times and centrifuged at 3,000 rpm for 3 min each; 20 µl of pretreated protein A agarose magnetic beads were added to the cell lysis buffer, and the tube was incubated with the antibody overnight and slowly shaken for 2-4 h at 4 °C to allow the antibody to couple with the protein A agarose magnetic beads. After the immunoprecipitation reaction, the agarose beads were centrifuged at 3,000× g for 3 min at 4 °C to precipitate them at the bottom of the tube. The supernatant was carefully removed, and the agarose magnetic beads were washed 3-4 times with 1 ml of lysis buffer, and the immunoprecipitation (IP) and IgG samples were prepared. The input, IP and IgG samples were prepared for the MS assay.

MS analysis was conducted by Shanghai GeneChem Co., Ltd. (Shanghai, China). MaxQuant 1.6.1.0 (AB Sciex, USA) and the UniProt Protein Database were also used for MS data analyses and protein comparative analysis. After mass spectrometry data retrieval, PSM FDR ≤ 0.01 and protein FDR ≤ 0.01 were used as the screening criteria for the peptide and protein identification, respectively. Peptide, razor+unique peptide, unique peptide, and sequence coverage (%) were counted together and separately in a protein identification table. If the sequence coverage of a protein in a sample was 0, then the protein was not identified in the sample. The input, IP and IgG samples were analyzed by WB as described.

**Co-IP assay.** Co-immunoprecipitation was conducted to identify the interactions between CCDC86 and NPM1 in NPC cell lines. CCDC86 and interacting proteins were co-immunoprecipitated from whole CNE2Z and 5-8F cell line extracts via a Protein A/G immunoprecipitation kit and standard co-IP experiments. Then, the immunocomplex was detected using a WB analysis according to the manufacturer's instructions. Detailed information on the antibodies for co-IP used in this study is shown in Supplementary Table S2.

**In vivo metastatic tumor experiment.** Ten healthy, 4-week-old female BALB/c nude mice were selected and purchased from Shanghai Ling Chang Biotechnology Co., Ltd. (SCXK (Shanghai) 2013-0018) and raised in the Animal Science Laboratory Department of Nanchang University Medical School under SPF laboratory animal conditions and in accordance with the relevant guidelines and regulations for the care and use of laboratory animals. The animal experiments in this study were approved by the Ethics Committee of the Second Affiliated Hospital of Nanchang University. All the methods were carried out in accordance with the approved guidelines. 5-8F cells transfected with sh-CCDC86 and sh-NC stably expressing luciferase were selected by 2 µg/ml puromycin to establish the metastatic tumor model *in vivo*. A total of 2×10<sup>7</sup> cells/ml of the cell suspension was prepared, and the cells were taken up with a disposable sterile syringe and slowly injected into the tail veins of nude

mice (200 µl in each mouse). According to methods used in previous studies [15, 16], and the general procedure of *in vivo* imaging is as follows: D-luciferin (AAT Bioquest) potassium working solution was prepared with sterile PBS at a concentration of 15 mg/ml sterilized and filtered through a 0.2 µm filter membrane. The D-luciferin potassium working solution was injected into nude mice at a dose of 10 µl/g. Fifteen minutes later, 0.7% pentobarbital sodium was injected into the intraperitoneal cavity of the nude mice at a dose of 10 µl/g to anesthetize the nude mice. A few minutes later, the nude mice were placed under a noninvasive *in vivo* bioluminescence imaging system (IVIS Lumina Series III, PerkinElmer, USA) to observe fluorescence, which was measured once per week. The experiment ended 51 days after inoculation, and *in vivo* imaging of the mice was performed before the end of the experiment.

**Statistical analysis.** The data are presented as the mean ± SD after analysis with SPSS Statistics software version 20 (SPSS Inc., USA). NPC patient survival association with the CCDC86 expression level was analyzed with the Kaplan-Meier method. Differences between groups were analyzed by Student's t-test or the nonparametric Mann-Whitney U test. A value of p < 0.05 was considered significant.

## Results

**CCDC86 is overexpressed in NPC.** As we know, CNE1 is a highly differentiated squamous cell carcinoma cell line of NPC. CNE2 and HONE1 are poorly differentiated squamous cell carcinoma cell lines of NPC. 5-8F is also a poorly differentiated squamous cell carcinoma cell line of NPC, which has high metastasis and high tumorigenic capacity. CNE2Z cell line is different from the CNE2 cell line, which is also a poorly differentiated NPC cell line. 6-10B is a poorly differentiated squamous cell carcinoma cell line of NPC with high tumorigenic potential but it does not have metastatic properties. HK1 is a highly differentiated NPC cell line carrying the EBV gene.

We first investigated the transcription of CCDC86 in these seven NPC cell lines, HONE1, HK1, CNE1, CNE2, CNE2Z, 5-8F, and 6-10B cells, and two nonmalignant human nasopharyngeal epithelial cell lines, NP69 and NP460 cells. Except for the HONE1 and HK1 cells, most of the NPC cell lines showed a higher mRNA expression level of CCDC86 than NP69 cells (Figure 1).

Then, CCDC86 protein levels in NPC tissues and normal nasopharyngeal epithelium (NNE) were detected by IHC. CCDC86 was localized in the cytoplasm of cells and was highly expressed in NPC tissues (n=124) but was negligibly expressed in NNE tissues (n=50) (Figure 2).

Furthermore, we analyzed the correlation between CCDC86 expression level and clinicopathological traits in the 124 NPC patients with higher CCDC86 expression (value higher than 6, n=50) and those with lower CCDC86 expression (value at or lower than 6, n=74). As shown in

Table 1, CCDC86 protein expression was not associated with the clinical parameters of NPC patients, including sex, age, histological type, or tumor clinical stage. However, it was positively correlated with cervical lymph node metastasis, recurrence or distant metastasis, although the difference was not statistically significant. We separately analyzed the clinical parameters of III–IV patients, because patients with recurrent or metastatic NPC are usually stage III–IV patients, and the therapeutic failure of NPC is associated with a high recurrence rate and a tendency toward distant metastasis. As shown in Table 2, the expression of CCDC86 was higher in patients with positive cervical lymph node metastasis, but the difference was not statistically significant. However, the expression of CCDC86 was positively correlated with the recurrence or distant metastasis, and the difference was statistically significant ( $p=0.044$ ).

In addition, we also analyzed the relationship between the expression level of CCDC86 and the survival rate (including the overall survival rate and the progression-free survival rate) in NPC patients. As shown in Figure 3A, the progression-free survival rate was slightly higher in patients with lower CCDC86 expression than in those with higher CCDC86 expression, but there was no significant difference ( $p=0.225$ ). The overall survival rate of the CCDC86 high-expression group was not significantly different from that of the low-expression group ( $p=0.681$ ) (Figure 3B). Additionally, for stage III–IV patients, the results showed that the progression-free survival rate was higher in patients with lower CCDC86 expression than in those with higher CCDC86 expression, and the difference was statistically significant ( $p=0.044$ ) (Figure 3C). The overall survival rate of the CCDC86 high-expression group was not significantly different from that of the low-expression group ( $p=0.364$ ), as shown in Figure 3D.

**CCDC86 knockdown inhibits NPC cell growth, migration, and invasion *in vitro*.** To investigate the biological roles of CCDC86 in NPC cells, three sh-RNAs specific to CCDC86 were designed and transfected into CNE2Z and 5-8F cells to downregulate the expression of CCDC86. After transfection, WB analysis showed that CCDC86 protein expression was significantly reduced in the three transfection groups, and the transfection was effective (Figure 4A). The sh-RNA1 fragment was the most efficient for 5-8F, the sh-RNA2 fragment was the most efficient for CNE2Z. However, in summary, sh-RNA1 has a good knockdown efficiency for both cell lines. So, we chose the first interference fragment for the subsequent experiment. The CCK-8 assays showed that the cell proliferation rate of the CCDC86 knockdown group was significantly decreased compared with that of the control group (Figure 4B). The cell clone formation assay showed that the number of cell clones of the CCDC86 knockdown group was significantly lower than that of the control group (Figure 4C). The EdU assays showed that the proportion of EdU-positive cells of the CCDC86 knockdown group was significantly lower than that of the control group

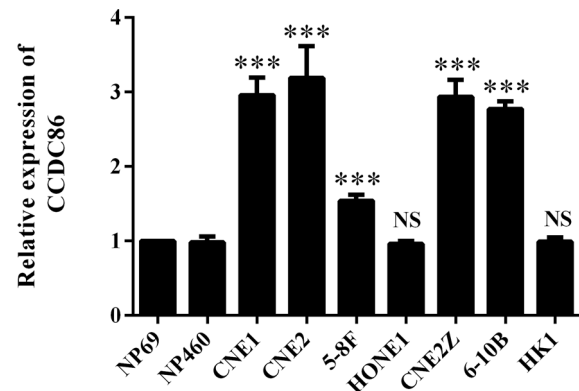


Figure 1. CCDC86 mRNA expression levels in nasopharyngeal carcinoma (NPC) cell lines and normal nasopharyngeal epithelial (NNE) cell lines. Real-time PCR of the mRNA expression levels of CCDC86 in 7 NPC cell lines and two noncancerous nasopharyngeal epithelial cell lines, NP69 and NP460 (NS: not significant; \*\*\* $p<0.001$ ).

Table 1. Correlations between the clinical characteristics and CCDC86 expression in NPC patients.

Clinicopathological features	Patients n=124	CCDC86 expression mean rank	p-value
Age(y)			0.550
<50	67	6.40±0.43	
≥50	57	6.00±0.52	
Gender			0.147
Male	94	5.89±0.39	
Female	30	7.03±0.65	
Clinical stages			0.461
I–II	69	6.39±0.46	
III–IV	55	5.89±0.49	
Lymph-node metastasis			0.789
+	98	6.23±0.39	
-	36	6.03±0.67	
Recurrence or distant metastasis			0.231
+	54	6.59±0.53	
-	70	5.79±0.42	
ΔNon-keratinizing carcinoma			0.882
Undifferentiated	107	6.05±0.37	
Differentiated	15	6.20±0.86	

\* $p<0.05$ ; ΔNote: Two of the 124 NPC patients had keratinized squamous cell carcinoma

Table 2. Correlations between the clinical characteristics and CCDC86 expression in NPC patients stage III–IV.

Clinicopathological features	Patients n=55	CCDC86 expression mean rank	p-value
Lymph-node metastasis			0.555
+	52	5.96±0.52	
-	3	4.67±0.67	
Recurrence or distant metastasis			0.044*
+	35	6.71±0.61	
-	20	4.70±0.72	

\* $p<0.05$

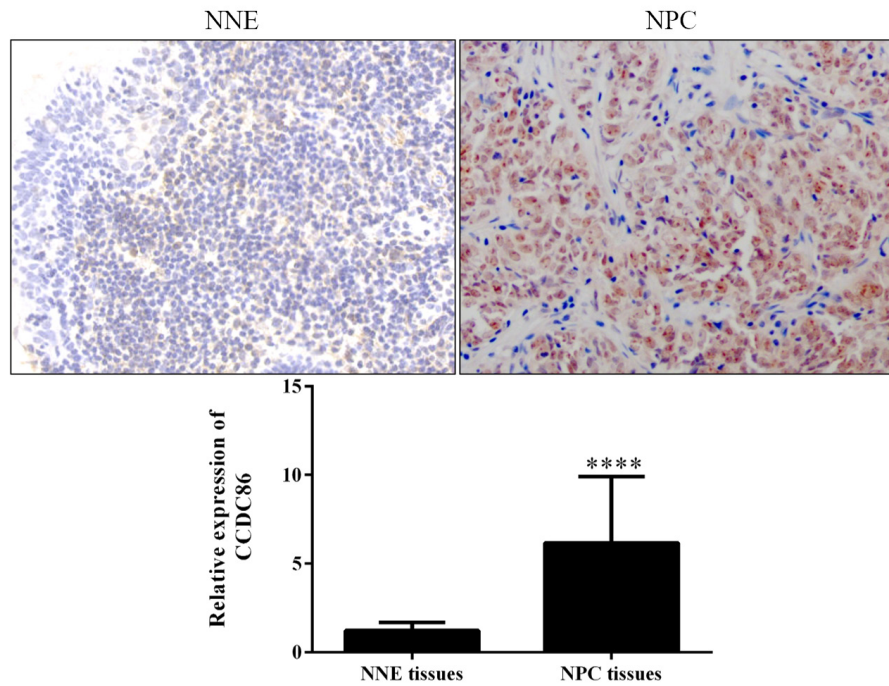


Figure 2. CCDC86 is overexpressed in NPC tissues. Immunohistochemical staining of CCDC86 in NPC (n=124) and NNE tissue (n=50). Representative images show immunostaining results for 1 NNE and 1 NPC sample (magnification  $\times 400$ ). The scored CCDC86 expression is shown in the bar graphs (\*\*\*\* $p < 0.0001$ ).

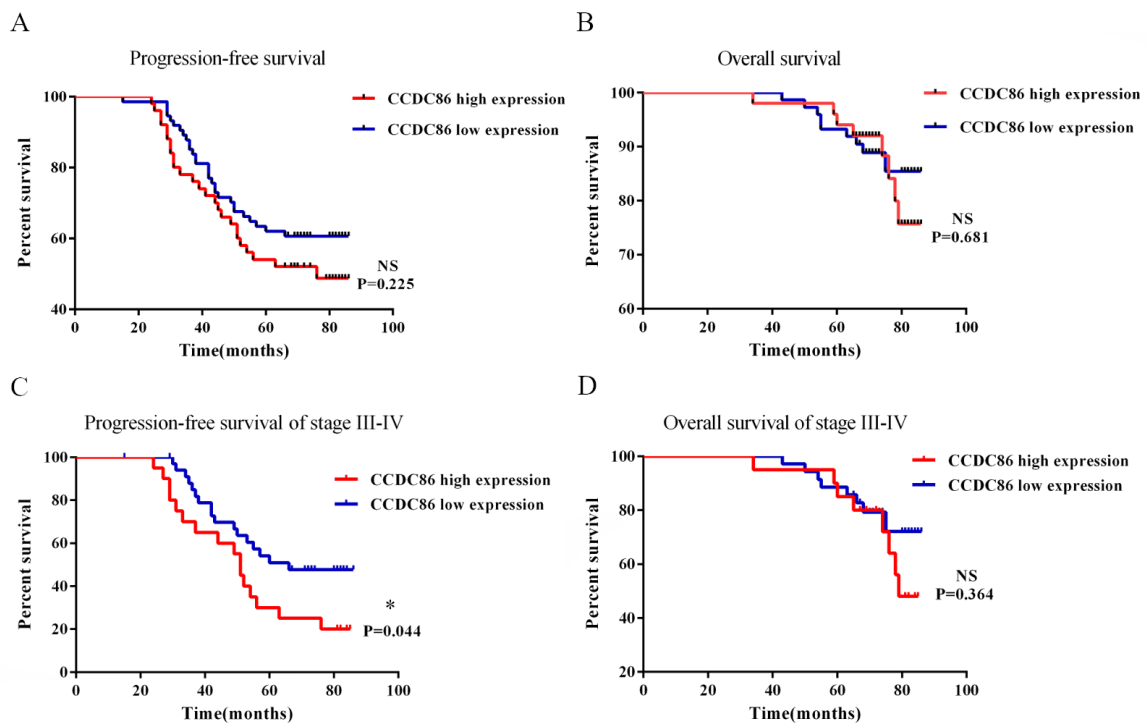
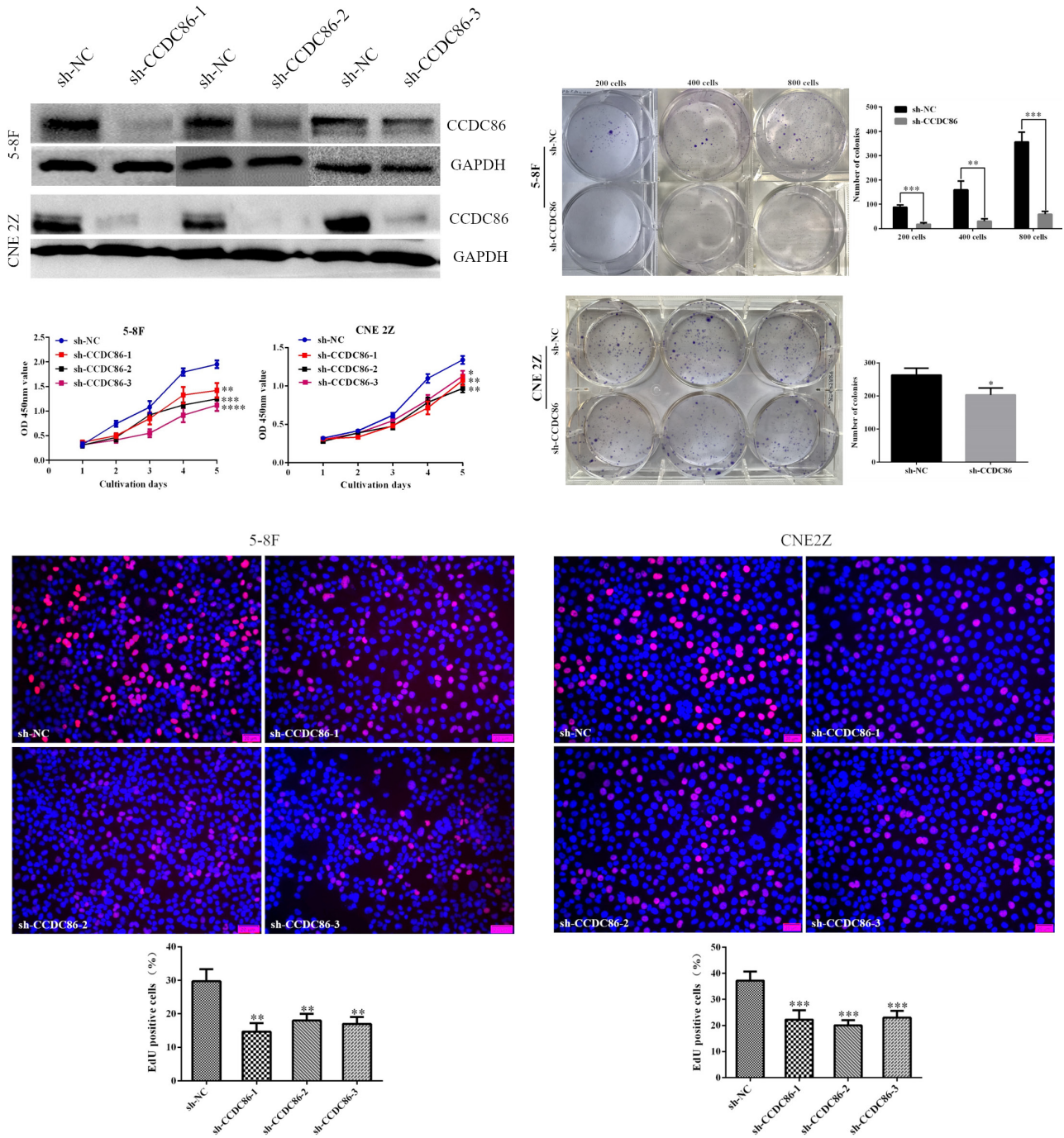


Figure 3. Relationship between CCDC86 expression and survival time in NPC patients. A) The progression-free survival rate was slightly better in patients with lower CCDC86 expression than in those with higher CCDC86 expression, but there was no significant difference ( $p=0.225$ ). B) The overall survival rate of the CCDC86 high-expression group was not significantly different from that of the low-expression group ( $p=0.681$ ). C) The progression-free survival rate was better in patients with lower CCDC86 expression than in those with higher CCDC86 expression in patients with stage III-IV disease, and the difference was statistically significant ( $p=0.044$ ). D) The overall survival rate of the CCDC86 high-expression group was still not significantly different from that of the low-expression group in the patients of stage III-IV ( $p=0.364$ ), \* $p < 0.05$ ; abbreviation: NS-not significant

(Figure 4D). Additionally, the wound-healing assay showed that the cell migration efficiency of the CCDC86 knockdown group was lower than that of the control group (Supplementary Figure S1A). Furthermore, Transwell migration

and invasion assays showed that the migrated and invasive cell numbers of 5-8F and CNE2Z cells with stable CCDC86 knockdown were much lower than those of control cells (Supplementary Figures S1B, S1C). Collectively, these data



**Figure 4.** CCDC86 knockdown inhibits NPC cell proliferation, migration, and invasion. A) Western blot confirmation of the silencing effect of the sh-CCDC86 construct in 5-8F and CNE2Z cell lines. B) The growth curves of 5-8F and CNE2Z cells with CCDC86 knockdown and their control cell lines were determined by CCK-8 assays. The data are presented as the mean ± SD of six independent experiments. C) Representative colony images and quantification of colonies in 5-8F and CNE2Z cells with and without CCDC86 knockdown. The data are presented as the mean ± SD of three independent experiments. D) Cell proliferation of 5-8F and CNE2Z cells with and without CCDC86 knockdown was determined by EdU incorporation assays (magnification 200×). The data are presented as the mean ± SD of three independent experiments. \*p<0.05, \*\*p<0.01, \*\*\*p<0.001, \*\*\*\*p<0.0001

demonstrated that CCDC86 knockdown inhibits NPC cell proliferation, migration, and invasion.

**CCDC86 overexpression enhances NPC cell growth, migration, and invasion *in vitro*.** To further validate the biological roles of CCDC86 in NPC, CCDC86 stably overexpressing 5-8F and CNE2Z cells were constructed via stable

transfection of a CCDC86 overexpression lentiviral vector, and the upregulated efficiency was also detected by WB analysis (Figure 5A). The CCK-8 assays showed that the cell proliferation rate in the CCDC86 overexpression group was significantly enhanced compared with that of the control group (Figure 5B). A cell clone formation assay showed

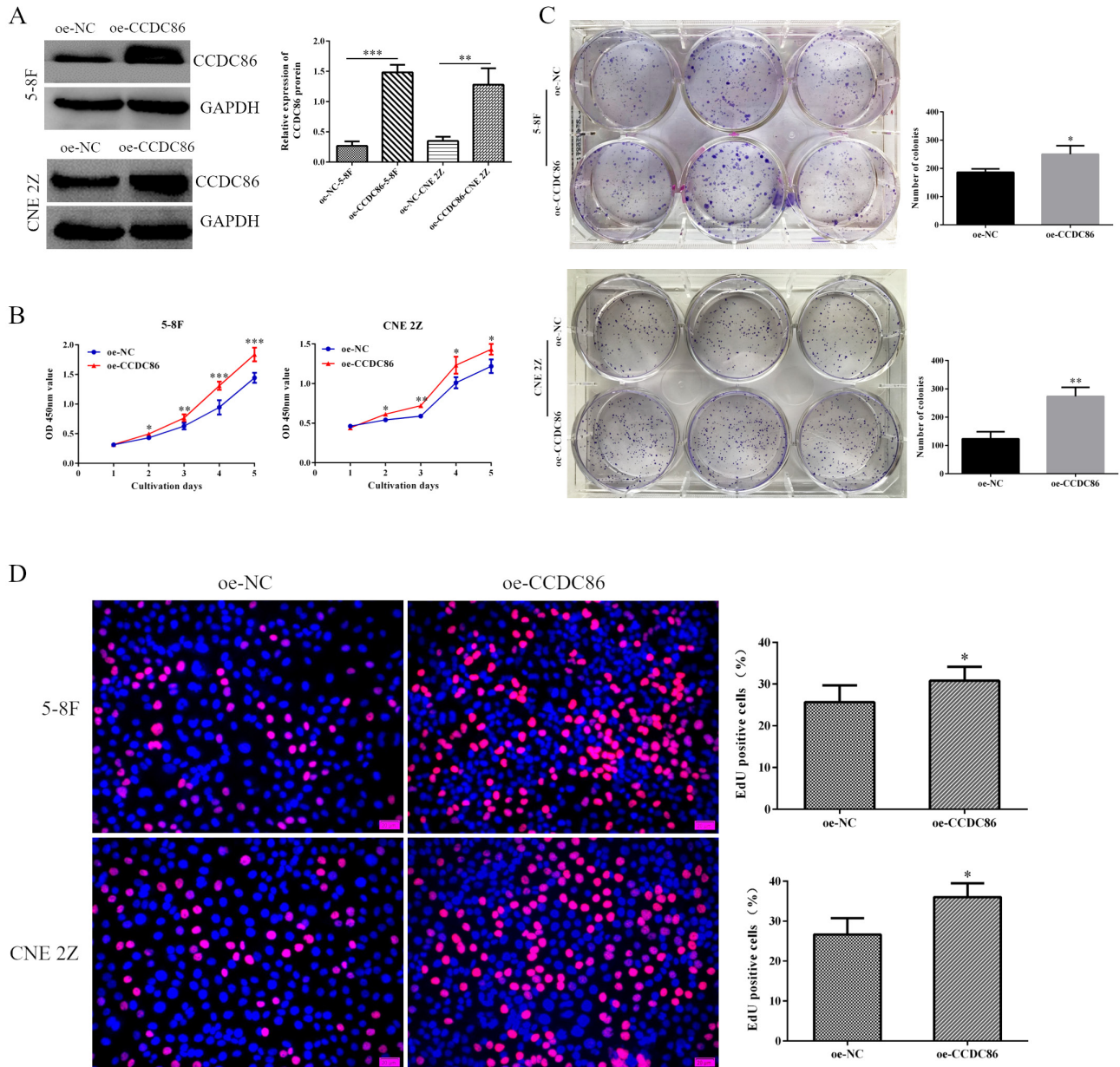


**Figure 5.** CCDC86 overexpression enhances NPC cell proliferation, migration, and invasion. **A)** The effects of overexpression in 5-8F and CNE2Z cell lines with CCDC86 overexpression were determined by Western blot analysis. **B)** The growth curves of 5-8F and CNE2Z cells with CCDC86 overexpression and their control cell lines were determined by CCK-8 assays. The data are presented as the mean  $\pm$  SD of six independent experiments. **C)** Colonies formed by 5-8F and CNE2Z cells with and without CCDC86 overexpression were quantified by colony formation assays. The data are presented as the mean  $\pm$  SD of three independent experiments. **D)** Proliferation of 5-8F and CNE2Z cells with and without CCDC86 overexpression was determined by EdU incorporation assays (magnification 200 $\times$ ). The data are presented as the mean  $\pm$  SD of three independent experiments. \* $p < 0.05$ , \*\* $p < 0.01$ , \*\*\* $p < 0.001$

that the number of cell clones in the CCDC86 overexpression group was significantly greater than that in the control group (Figure 5C). The EdU assays showed that the proportion of EdU-positive cells CCDC86 overexpression group was significantly greater than that of the control group (Figure 5D). Moreover, a wound-healing assay showed that the cell migration ability of the CCDC86 overexpression group was enhanced compared with that of the control group (Supplementary Figures S2A, S2B). Furthermore, Transwell migration and invasion assays showed that the migrated and invasive cell numbers of the CCDC86-stably-overexpressing 5-8F and CNE2Z cells were much greater than those of the control cells (Supplementary Figures S2C, S2D). Collectively, these data demonstrated that CCDC86 overexpression enhances NPC cell proliferation, migration, and invasion.

**CCDC86 knockdown inhibits the metastasis of NPC cells *in vivo*.** To further investigate the effect of CCDC86 on NPC metastasis, we designed a lung metastatic mouse model to verify that CCDC86 can promote NPC metastasis *in vivo*. The lung metastasis model of nude mice was established by 5-8F cells stably transfected with sh-CCDC86 and a luciferase expression construct and injected through the tail vein. The bioluminescence imaging system was used to detect the fluorescence of nude mice every week, and the results showed that the fluorescence of the CCDC86 knockdown group was lower than that of the control group (Figure 6C). The experiment ended 51 days after inoculation, and the nude mice were imaged *in vivo* before the end. The results also showed that the fluorescence of the CCDC86 knockdown group was lower than that of the control group. The

difference was statistically significant (Figures 6A, 6B) These results suggested that CCDC86 knockdown can inhibit the pulmonary metastasis of NPC cells *in vivo*.

**Knockdown of CCDC86 inhibits cell invasion and migration by reversing EMT and inhibiting MMPs.** To further evaluate whether CCDC86 can promote the invasion and migration of NPC cells by promoting the EMT process and increasing the expression of MMPs, the expression levels of EMT-related proteins (E-cadherin,  $\beta$ -catenin, and Vimentin), MMP9, and MMP2 in 5-8F and CNE2Z cells with CCDC86 knockdown and their control groups were detected by WB analysis. As shown in Figure 7, E-cadherin protein expression was upregulated in CCDC86 knockdown cells, while  $\beta$ -catenin, vimentin, MMP2, and MMP9 protein expression levels were downregulated. These results suggested that CCDC86 may be involved in the EMT process and mediate the expression of MMPs in NPC cell lines.

**CCDC86 is positively correlated with epidermal growth factor receptor (EGFR), a key upstream effector of Akt signaling.** We conducted gene chip screening and IPA (Ingenuity Pathway Analysis) to identify downstream genes or proteins of CCDC86. All genes in the PTEN pathway were mapped in a gene interaction network with the target gene CCDC86 (Figure 8A). Through this network and the IPA results, we found that CCDC86 is correlated with EGFR and might promote the malignant biological function of NPC cells through EGFR. To verify this prediction, we assessed the expression of EGFR at both the protein and mRNA levels. EGFR protein and mRNA were downregulated in cells with CCDC86 knocked down (Figures 8B, 8C).

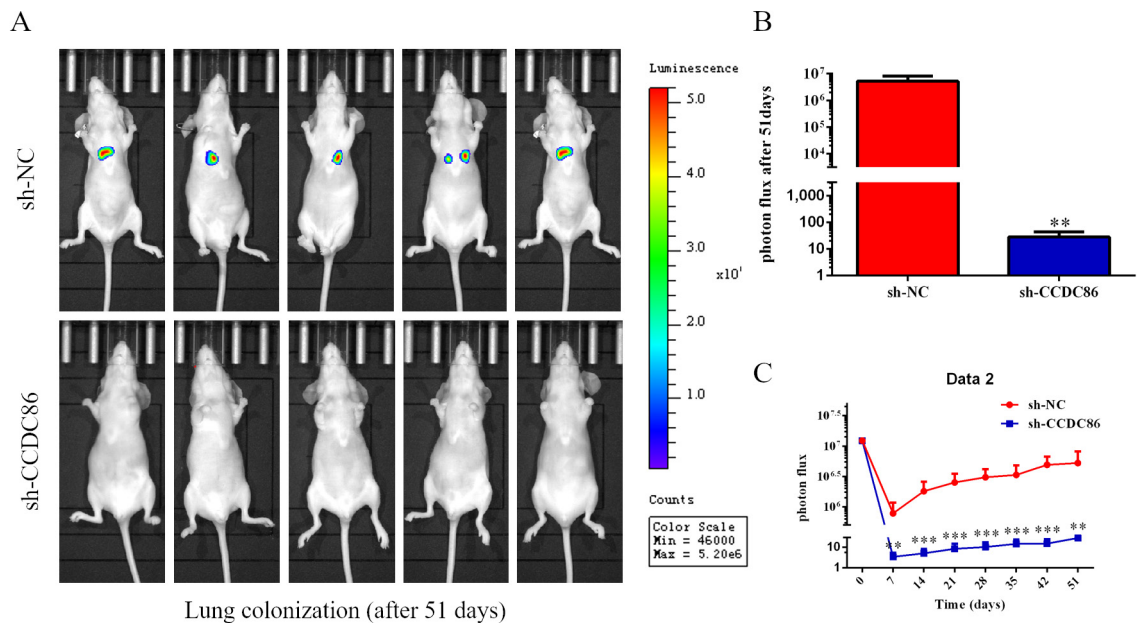


**Figure 6.** Knockdown of CCDC86 inhibits the metastasis of NPC cells *in vivo*. Compared with the control group, each week (C) and 51 days later (A, B), the bioluminescent signals were lower in the CCDC86 knockdown group. \*\* $p < 0.01$ , \*\*\* $p < 0.001$

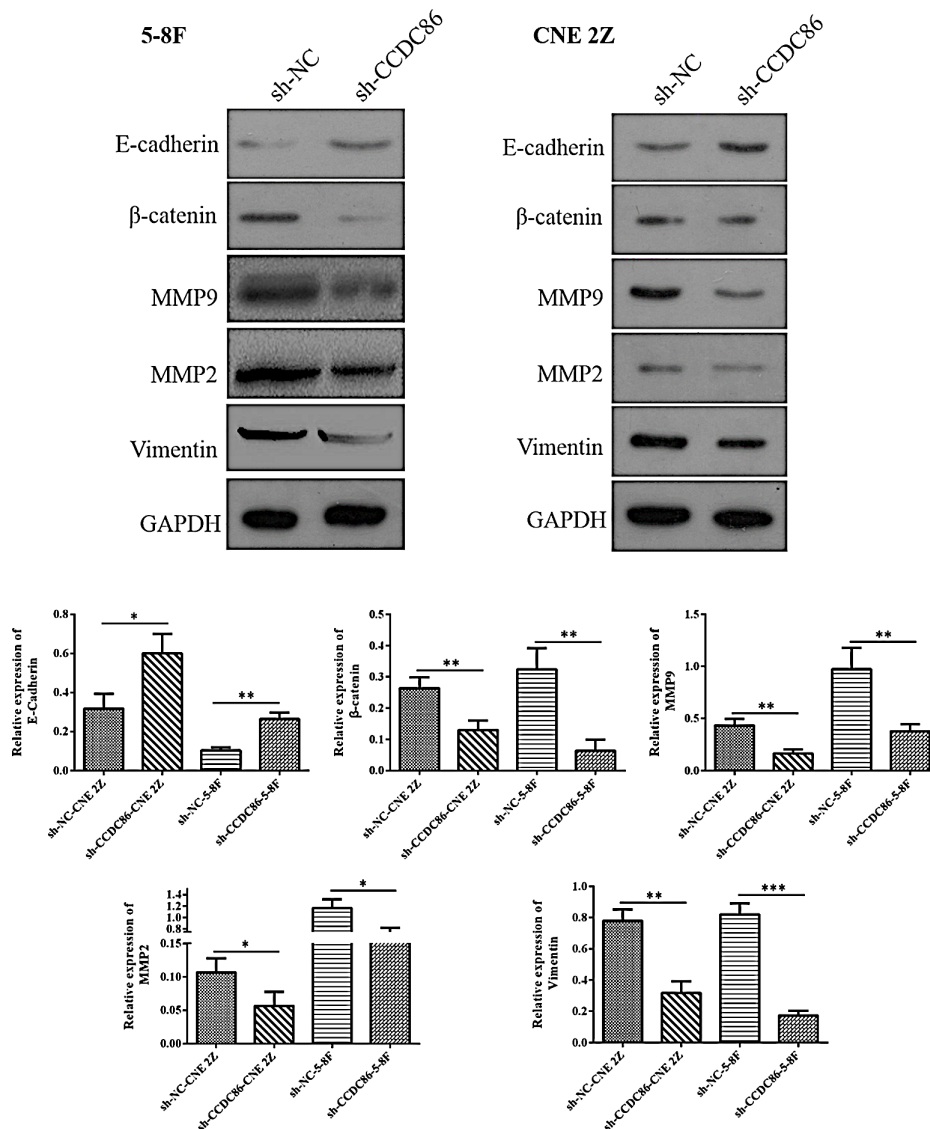


**Figure 7.** Knockdown of CCDC86 inhibits NPC cell migration and invasion by reversing the epithelial-mesenchymal transition (EMT) and promoting MMP expression. Western blot analysis of the expression of EMT-related proteins (E-cadherin, β-catenin, and Vimentin), MMP9, and MMP2. GAPDH was used as an internal control. The data are presented as the mean ± SD (n=3) \*p<0.05, \*\*p<0.01, \*\*\*p<0.001

These results showed that CCDC86 is positively correlated with EGFR and that CCDC86 can promote the expression of EGFR in NPC cell lines.

**CCDC86 promotes NPC cell metastasis by upregulating EGFR expression.** Considering these results, we attempted to determine whether EGFR is involved in the malignant biological function promotion of CCDC86 in NPC cells. Four groups of sh-CCDC86, sh-NC, sh-CCDC86+EGF, and sh-NC+EGF cells were constructed, and a series of functional assays were performed to verify this hypothesis. The cell proliferation experiment results showed that downregulation of CCDC86 could inhibit the proliferation of NPC cells, although overexpression of EGFR could reverse this inhibitory effect (Figures 9A, 9B). The same results

were observed in the cell invasion assay (Figure 9C). These findings suggested that in the process of CCDC86 promoting the proliferation, invasion, and migration of NPC cells, EGFR is a key downstream target gene. That is, CCDC86 promotes NPC progression by upregulating EGFR.

**Knockdown of CCDC86 suppresses EGFR to inhibit the PI3K/Akt signaling pathway.** These results confirmed that CCDC86 promoted the proliferation, invasion, and migration of NPC cells by upregulating EGFR. However, the downstream signaling pathway remained unclear. Therefore, we explored the signaling pathway in the next experiments. Multiple studies have proven that the PI3K/Akt pathway plays important roles in the process of tumorigenesis, such as promoting proliferation, EMT, and angiogenesis [17].

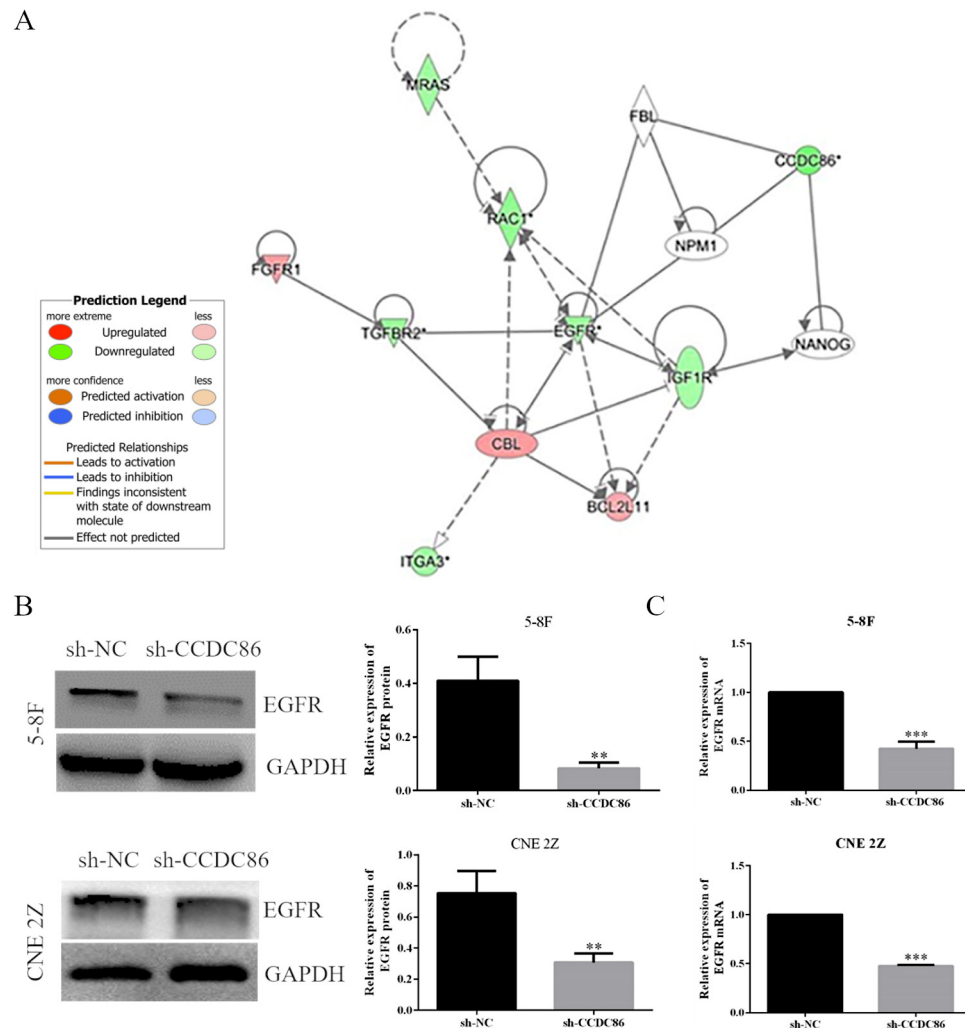


**Figure 8.** CCDC86 is positively correlated with EGFR. A) All genes in the PTEN pathway were mapped in a gene interaction network with the target gene CCDC86. B) EGFR protein levels in the negative control and CCDC86-knockdown cell lines were determined by Western blot analysis. C) Relative expression of EGFR at the mRNA level in the negative control and CCDC86 knockdown cell lines was determined by qRT-PCR. GAPDH was used as an internal control.

The PI3K/Akt pathway is a classical downstream pathway of EGFR and the most important pathway in head and neck squamous cell carcinoma [18]. To clarify whether the PI3K/Akt signaling pathway is involved in mediating the effects of CCDC86 on NPC, the protein expression levels of PI3K and Akt and their levels of phosphorylation were detected by WB assay. As shown in Figure 9D, the levels of PI3K and Akt phosphorylation were decreased in NPC cell lines with CCDC86 knocked down, but this inhibitory effect was reversed by overexpression of EGFR.

Taken together, these data suggested that the knockdown of CCDC86 suppresses the PI3K/Akt signaling pathway by negatively regulating the expression of EGFR, thereby inhibiting the proliferation, invasion, and migration of NPC cells. In other words, CCDC86 promotes the proliferation, invasion, and migration of NPC cells by upregulating the

expression of EGFR and activating the PI3K/Akt signaling pathway.

**CCDC86 promotes EGFR expression by mediating NPM1.** To determine whether CCDC86 directly regulates EGFR and affects the malignant biological function of NPC cells, we designed a MS assay to identify downstream proteins that bind directly to CCDC86. The base peak of the mass spectrum is shown in Supplementary Figure S3. Peptide, razor+unique peptide, unique peptide, and sequence coverage (%) were combined and separately counted in the protein identification table. If the sequence coverage of a protein in a sample was 0, the protein had not been identified in the sample; that is, the protein did not bind directly to the target protein. As shown in Table 3, the sequence coverage (%) of EGFR was 0, but the sequence coverage (%) of NPM1 and FBL was not 0. These results

**Table 3. Protein identification results.**

Protein names	Epidermal growth factor receptor	Nucleophosmin	rRNA 2-O-methyltransferase fibrillar
Gene names	EGFR	NPM1	FBL
Peptide	26	16	11
Razor + unique peptides	26	16	11
Unique peptides	26	16	10
Sequence coverage [%]	33	55.1	51.2
Sequence coverage IgG [%]	0	27.9	17.3
Sequence coverage Input [%]	33	55.1	43.5
Sequence coverage IP [%]	0	33	24.6

indicated that EGFR did not directly bind to CCDC86, while FBL and NPM1 might directly bind to CCDC86. According to the results shown in the previous gene interaction network diagram (Figure 8A), NPM1 is downstream of CCDC86; therefore, we speculated that NPM1 directly binds to CCDC86 and might be involved in the process by which CCDC86 regulates EGFR. Considering these results, we used a co-IP assay to verify whether CCDC86 can directly bind to NPM1. The immunoblot results indicated that the NPM1 proteins of CCDC86 were enriched in the pulldown and input samples. In contrast, CCDC86 and interacting proteins were not identified with IgG. These results demonstrated that the method was efficient, specifically co-immunoprecipitating CCDC86 and its interacting NPM1 protein partner in CNE2Z and 5-8F cell lines. These results confirmed the interaction between CCDC86 and NPM1 (Figure 9E). They also suggested that CCDC86 may positively regulate EGFR by mediating NPM1, thus promoting the proliferation, invasion, and migration of NPC cells.

## Discussion

In 2015, there were 60,600 confirmed cases of NPC in China, accounting for approximately 1.41% of the total incidence of malignant tumors [19]. NPC has obvious regional and ethnic distribution characteristics [20]. It is highly prevalent in southern China and Southeast Asian countries, of which Guangdong, Guangxi, Hunan, Fujian, and Jiangxi provinces are the core regions [21]. Although the overall 5-year survival rate for NPC is as high as 75–80%, local recurrence and distant metastasis occur in nearly 10–15% of patients within the first 2 years after the initiation of NPC treatment, and only 72.9% of patients have 2-year progression-free survival [22]. Therefore, it is necessary to investigate the molecular mechanisms underlying metastatic NPC and to identify novel targets for metastasis prevention and therapy.

The analysis of clinical parameters was based on 124 NPC patients and showed that there was no significant correlation between CCDC86 expression level and clinical

parameters such as sex, age, histological type, and clinical stage. However, the CCDC86 expression level was positively correlated with cervical lymph node metastasis, recurrence, and distant metastasis, although the difference was not statistically significant; this negative result is worthy of further discussion. Therefore, stage III–IV patients were selected for analysis, and the results showed that CCDC86 expression was higher in patients with positive cervical lymph node metastasis, although the difference was not statistically significant. We found that these negative results were related to the low number of patients with negative lymph node metastasis in stage III–IV (n=3). However, the CCDC86 expression level was positively correlated with the recurrence or distant metastasis of patients, and the difference was statistically significant. Therefore, we believe that the CCDC86 expression level can affect the prognosis of patients with advanced NPC.

In addition, we found that CCDC86 was associated with shorter recurrence-free survival time in NPC patients, especially in stage III–IV patients, which was consistent with the results described above. It was also suggested that CCDC86 may be a new risk biomarker for the prognosis of advanced NPC. However, the CCDC86 expression level was not significantly associated with overall survival in NPC patients at all stages or in patients with III–IV disease. We found that this result may have been related to the relatively high overall 5-year survival rate of NPC patients, with only 17 deaths occurring among 124 patients during our total follow-up period of 86 months.

It is well known that therapeutic failure of NPC is associated with a high recurrence rate and a tendency toward distant metastasis. Therefore, those performing basic research need to pay more attention to tumor metastasis, and studies of the mechanism of tumor metastasis are urgently needed. Our functional experiments demonstrated that CCDC86 promotes NPC cell proliferation, migration, and invasion *in vitro* and *in vivo*. CCDC86 might be a putative oncogene modulating tumor proliferation and metastasis in NPC. However, how does CCDC86 mediate the invasion and migration of NPC cells to promote tumor metastasis? To answer this question, we shifted our attention to the

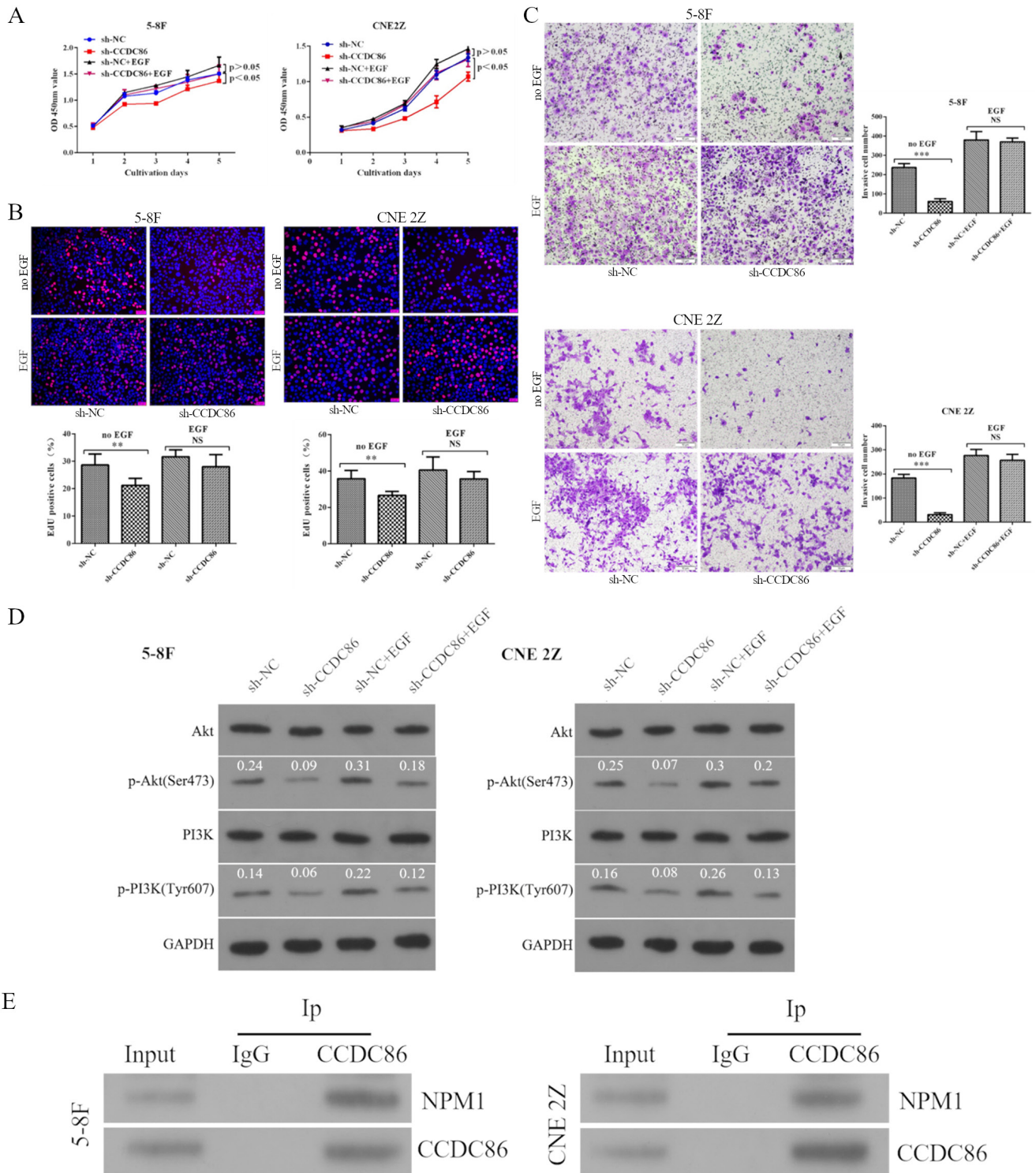


**Figure 9.** A) The growth curves of 5-8F and CNE2Z cells with and without CCDC86 knockdown and cells cultured with EGF were determined by CCK-8 assays. B) Proliferation of 5-8F and CNE2Z cells with and without CCDC86 knockdown and cells cultured with EGF was determined by EdU incorporation assays (magnification 200 $\times$ ). C) Invasion of stable CCDC86-knockdown 5-8F/CNE2Z cells cultured with EGF was determined by Transwell invasion assays (magnification 200 $\times$ ). The data are presented as the mean  $\pm$  SD of three independent experiments (\*\* $p < 0.01$ , \*\*\* $p < 0.001$ , NS: not significant). D) Knockdown of CCDC86 suppresses EGFR to inhibit the PI3K/Akt signaling pathway. Western blot analysis of the indicated proteins in 5-8F and CNE2Z cells with and without CCDC86 knocked down, and cells cultured with EGF. GAPDH was used as an internal control. E) Co-IP assay analysis of the interactions between CCDC86 and NPM1 in 5-8F and CNE2Z cells. The NPM1 proteins interacting with CCDC86 in the 5-8F and CNE2Z cell lines were enriched in the pull-down assay with input samples but were not identified with IgG.

EMT and MMPs. Is the role of CCDC86 in the invasion and migration of NPC cells involved in the regulation of MMPs and the EMT process? In this study, we used WB analyses to detect changes in the EMT-related proteins (E-cadherin,  $\beta$ -catenin, and Vimentin), MMP2, and MMP9 after CCDC86 knockdown. The results suggested that the knockdown of CCDC86 can inhibit the protein expression of MMP2 and MMP9 and reverse the EMT process of NPC cells. In other words, CCDC86 can promote cell invasion and migration by enhancing the EMT process and upregulating the expression of MMP2 and MMP9.

Metastasis is an important factor in determining the prognosis and survival of NPC patients. Therefore, we further explored the specific mechanism of CCDC86 in NPC. Through gene chip screening and IPA analysis, we found that CCDC86 and EGFR may have a certain interaction relationship that is worthy of further study. Our results confirmed that the mRNA and protein expression levels of EGFR are significantly downregulated after the knockdown of CCDC86 in NPC cells. EGFR is a key upstream regulatory protein of the PI3K/Akt pathway. Previous studies have shown that inhibition of the EGFR-PI3K/Akt pathway can induce NPC cell senescence and inhibit the tumor stem cell phenotype [23, 24].

EGF is a ligand of EGFR, and the binding of the extracellular domain of EGFR to EGF leads to the autophosphorylation of EGFR, which can simultaneously activate the downstream signaling pathway to cause specific physiological effects [25]. Therefore, we used EGF as the activator of EGFR to conduct a series of studies. According to previous research [26], an EGF concentration of 100 ng/ml and an action time of 24 h are the best experimental conditions. Our results suggested that the promotion of CCDC86 on the malignant biological function of NPC cells depends on the upregulation of EGFR expression. Therefore, these results confirm that EGFR is an important intermediate target gene of CCDC86 acting on NPC. Then, we further explored the signaling pathway involved in the regulation of EGFR by CCDC86 for the malignant biological function of NPC cells. The results showed that the expression of p-PI3K and p-AKT is downregulated after CCDC86 knockdown, but these results can be reversed by EGFR overexpression. These results suggest that the EGFR-mediated PI3K/Akt signaling pathway is indeed involved in the process by which CCDC86 acts on NPC. In other words, CCDC86 promotes NPC metastasis by positively regulating EGFR expression and then activating the PI3K signaling pathway.

Nucleophosmin (NPM, B23) is an important protein molecule located in the particle region of nucleoli and includes NPM1, NPM2, NPM3, and three other subtypes. Currently, research on NPM1 is more in-depth; therefore, NPM1 is commonly known as NPM. Under physiological conditions, NPM is widely expressed in cells in various tissues and is related to a variety of important biological functions of cells [27, 28]. The expression level of NPM is

directly proportional to cell proliferation, and its expression level in tumor cells and proliferative cells has been previously shown to be significantly higher than that in quiescent cells [29–31]. NPM1 is the most frequently occurring genetic abnormality in acute myeloid leukemia and can participate in the malignant proliferation and transformation of leukemia cells in various ways [32–35]. Another study recently revealed that nucleophosmin 1 (NPM1) mutation is considered a Class II mutation affecting hematopoietic transcription and differentiation [36]. There are few studies on the relationship between CCDC86 and NPM1, but as shown in previous studies, CCDC86 is related to the occurrence of lymphoma [3], and both play important roles in the occurrence of tumors in the blood system and may have an unrevealed relationship.

There have been more studies on the correlation between NPM1 and EGFR. Overexpression of EGFR in solid tumors has been confirmed in several studies, but there are few data available on hematological malignancies such as AML. Sun *et al.* showed that from M1 to M7 subtypes, EGFR expression was approximately 33% in AML, and high EGFR expression was associated with the poor prognosis of AML [37]. EGFR expression was significantly higher in patients with wild-type NPM1 than in patients with mutated NPM1 in acute myeloid leukemia patients of Assam, India ( $p < 0.01$ ) [38]. These results suggested that CCDC86, EGFR, and NPM1 interact with each other to varying degrees in the pathogenesis of hematological tumors. Therefore, we believe that the interactions among these three proteins may also be involved in the pathogenesis of NPC. Our results also indicated that CCDC86 directly regulates NPM1 but not EGFR, and CCDC86 may positively regulate EGFR by mediating NPM1, promoting the activation of PI3K/Akt signaling and the proliferation, invasion, and migration of NPC cells. However, the specific mechanism by which CCDC86 directly regulates NPM1 is not yet clear. Whether CCDC86 regulates its expression level or causes its mutation is not known and will require further research in the future.

In summary, our study shows that CCDC86 is overexpressed in NPC cells and tumor tissues. CCDC86 promoted cell proliferation, enhanced EMT, and promoted NPC cell invasion and migration via PI3K/Akt signaling by mediating NPM1, and then positively regulating EGFR to modulate metastasis in NPC. Thus, CCDC86 may serve as a potential treatment target in metastatic NPC.

**Supplementary information** is available in the online version of the paper.

**Acknowledgments:** The study was supported by the Natural Science Foundation of Jiangxi Province (Grant No.20232BAB216060 and 20224BAB206049), the National Natural Science Foundation project (Grant No.81960190), and the National Natural Science Foundation incubation project of the Second Affiliated Hospital of Nanchang University (Grant No.2021YNFY12016).

## References

- [1] BRAY F, FERLAY J, SOERJOMATARAM I, SIEGEL RL, TORRE LA et al. Global cancer statistics 2018: GLOBOCAN estimates of incidence and mortality worldwide for 36 cancers in 185 countries. *CA Cancer J Clin* 2018; 68: 394–424. <https://doi.org/10.3322/caac.21492>
- [2] BUSSEY KA, LAU U. The interferon-stimulated gene product oligoadenylate synthetase-like protein enhances replication of Kaposi's sarcoma-associated herpesvirus (KSHV) and interacts with the KSHV ORF20 protein. *PLoS Pathol* 2018; 14: e1006937. <https://doi.org/10.1371/journal.ppat.1006937>
- [3] ZHANG J, MEDEIROS LJ, YOUNG KH. Cancer Immunotherapy in Diffuse Large B-Cell Lymphoma. *Front Oncol* 2018; 8: 351. <https://doi.org/10.3389/fonc.2018.00351>
- [4] JIA Y, YUN CH, PARK E, ERCAN D, MANUIA M et al. Overcoming EGFR(T790M) and EGFR(C797S) resistance with mutant-selective allosteric inhibitors. *Nature* 2016; 534: 129–132. <https://doi.org/10.1038/nature17960>
- [5] MOHAMMED AA, EL-TANNI H, EL-KHATIB HM, MIRZA AA, MIRZA AA et al. Urinary Bladder Cancer: Biomarkers and Target Therapy, New Era for More Attention. *Oncol Rev* 2016; 10: 320. <https://doi.org/10.4081/oncol.2016.320>
- [6] GAO Y, MA YC, JU YH, LI YN. Mosaicism trisomy 10 in a 14-month-old child with additional neurological abnormalities: case report and literature review. *BMC Pediatr* 2018; 18: 266. <https://doi.org/10.1186/s12887-018-1237-1>
- [7] ZHANG G, AN Y, LU X, ZHONG H, ZHU Y et al. A Novel Naphthalimide Compound Restores p53 Function in Non-small Cell Lung Cancer by Reorganizing the Bak-Bcl-xl Complex and Triggering Transcriptional Regulation. *J Biol Chem* 2016; 291: 4211–4225. <https://doi.org/10.1074/jbc.M115.669978>
- [8] CHEN S, QIU Y, GUO P, PU T, FENG Y et al. FGFR1 and HER1 or HER2 co-amplification in breast cancer indicate poor prognosis. *Oncol Lett* 2018; 15: 8206–8214. <https://doi.org/10.3892/ol.2018.8423>
- [9] SIKDAR N, SAHA G, DUTTA A, GHOSH S, SHRIKHANDE SV et al. Genetic Alterations of Periampullary and Pancreatic Ductal Adenocarcinoma: An Overview. *Curr Genomics* 2018; 19: 444–463. <https://doi.org/10.2174/1389202919666180221160753>
- [10] HUANG Y, CHENG C, ZHANG C, ZHANG Y, CHEN M et al. Advances in prostate cancer research models: From transgenic mice to tumor xenografting models. *Asian J Urol* 2016; 3: 64–74. <https://doi.org/10.1016/j.ajur.2016.02.004>
- [11] LIN Q, WANG H, LIN X, ZHANG W, HUANG S et al. PTPN12 Affects Nasopharyngeal Carcinoma Cell Proliferation and Migration Through Regulating EGFR. *Cancer Biother Radiopharm* 2018; 33: 60–64. <https://doi.org/10.1089/cbr.2017.2254>
- [12] ZHAO Z, GAO D, MA T, ZHANG L. MicroRNA-141 suppresses growth and metastatic potential of head and neck squamous cell carcinoma. *Aging (Albany NY)* 2019; 11: 921–932. <https://doi.org/10.18632/aging.101791>
- [13] DAI N, YE R, HE Q, GUO P, CHEN H et al. Capsaicin and sorafenib combination treatment exerts synergistic anti-hepatocellular carcinoma activity by suppressing EGFR and PI3K/Akt/mTOR signaling. *Oncol Rep* 2018; 40: 3235–3248. <https://doi.org/10.3892/or.2018.6754>
- [14] JIANG W, TIAN W, IJAZ M, WANG F. Inhibition of EGF-induced migration and invasion by sulfated polysaccharide of *Sepiella maindroni* ink via the suppression of EGFR/Akt/p38 MAPK/MMP-2 signaling pathway in KB cells. *Biomed Pharmacother* 2017; 95: 95–102. <https://doi.org/10.1016/j.biopha.2017.08.050>
- [15] HO MY, LIANG SM, HUNG SW, LIANG CM. MIG-7 controls COX-2/PGE2-mediated lung cancer metastasis. *Cancer Res* 2013; 73: 439–449. <https://doi.org/10.1158/0008-5472.can-12-2220>
- [16] ABDULGHANI J, GU L, DAGVADORJ A, LUTZ J, LEIBY B et al. Stat3 promotes metastatic progression of prostate cancer. *Am J Pathol* 2008; 172: 1717–1728. <https://doi.org/10.2353/ajpath.2008.071054>
- [17] CHENG GZ, PARK S, SHU S, HE L, KONG W et al. Advances of AKT pathway in human oncogenesis and as a target for anti-cancer drug discovery. *Curr Cancer Drug Targets* 2008; 8: 2–6.
- [18] PSYRRI A, SEIWERT TY, JIMENO A. Molecular pathways in head and neck cancer: EGFR, PI3K, and more. *Am Soc Clin Oncol Educ Book* 2013; 246–255. [https://doi.org/10.14694/EdBook\\_AM.2013.33.246](https://doi.org/10.14694/EdBook_AM.2013.33.246)
- [19] CHEN W, ZHENG R, BAADE PD, ZHANG S, ZENG H et al. Cancer statistics in China, 2015. *CA Cancer J Clin* 2016; 66: 115–132. <https://doi.org/10.3322/caac.21338>
- [20] CHEN YP, CHAN ATC, LE QT, BLANCHARD P, SUN Y et al. Nasopharyngeal carcinoma. *Lancet* 2019; 394: 64–80. [https://doi.org/10.1016/s0140-6736\(19\)30956-0](https://doi.org/10.1016/s0140-6736(19)30956-0)
- [21] SUWINSKI P, ONG C, LING MHT, POH YM, KHAN AM et al. Advancing Personalized Medicine Through the Application of Whole Exome Sequencing and Big Data Analytics. *Front Genet* 2019; 10: 49. <https://doi.org/10.3389/fgene.2019.00049>
- [22] LIAN J, LI Y, YU M. MicroRNA-183 and microRNA-141 are potential risk factors for poor prognosis in patients with nasopharyngeal carcinoma. *Oncol Lett* 2019; 17: 1172–1176. <https://doi.org/10.3892/ol.2018.9650>
- [23] CHAN KC, TING CM, CHAN PS, LO MC, LO KW et al. A novel Hsp90 inhibitor AT13387 induces senescence in EBV-positive nasopharyngeal carcinoma cells and suppresses tumor formation. *Mol Cancer* 2013; 12: 128. <https://doi.org/10.1186/1476-4598-12-128>
- [24] MA L, ZHANG G, MIAO XB, DENG XB, WU Y et al. Cancer stem-like cell properties are regulated by EGFR/AKT/ $\beta$ -catenin signaling and preferentially inhibited by gefitinib in nasopharyngeal carcinoma. *FEBS J* 2013; 280: 2027–2041. <https://doi.org/10.1111/febs.12226>
- [25] PHILIPPAR U, ROUSSOS ET, OSER M, YAMAGUCHI H, KIM HD et al. A Mena invasion isoform potentiates EGF-induced carcinoma cell invasion and metastasis. *Dev Cell* 2008; 15: 813–828. <https://doi.org/10.1016/j.devcel.2008.09.003>

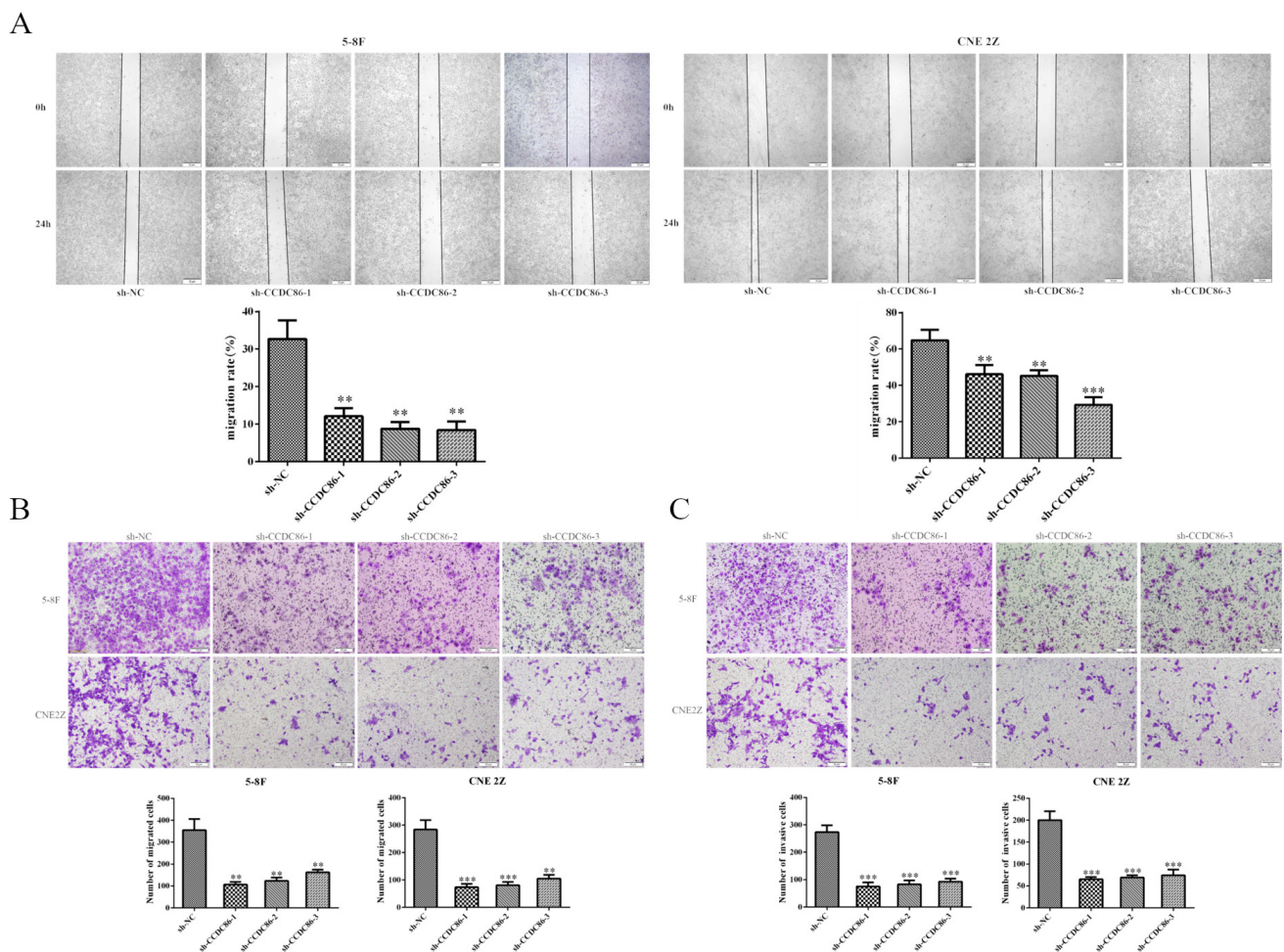
- [26] JIANG W, CHENG Y, ZHAO N, LI L, SHI Y et al. Sulfated polysaccharide of *Sepiella Maindroni* ink inhibits the migration, invasion and matrix metalloproteinase-2 expression through suppressing EGFR-mediated p38/MAPK and PI3K/Akt/mTOR signaling pathways in SKOV-3 cells. *Int J Biol Macromol* 2018; 107: 349–362. <https://doi.org/10.1016/j.ijbiomac.2017.08.178>
- [27] LIM MJ, WANG XW. Nucleophosmin and human cancer. *Cancer Detect Prev* 2006; 30: 481–490. <https://doi.org/10.1016/j.cdp.2006.10.008>
- [28] BOX JK, PAQUET N, ADAMS MN, BOUCHER D, BOLDEPERSON E et al. Nucleophosmin: from structure and function to disease development. *BMC Mol Biol* 2016; 17: 19. <https://doi.org/10.1186/s12867-016-0073-9>
- [29] COLOMBO E, ALCALAY M, PELICCI PG. Nucleophosmin and its complex network: a possible therapeutic target in hematological diseases. *Oncogene* 2011; 30: 2595–2609. <https://doi.org/10.1038/onc.2010.646>
- [30] WANG H, YUAN G, ZHAO B, ZHAO Y, QIU Y. High expression of B23 is associated with tumorigenesis and poor prognosis in bladder urothelial carcinoma. *Mol Med Rep* 2017; 15: 743–749. <https://doi.org/10.3892/mmr.2016.6033>
- [31] TSUI KH, CHENG AJ, CHANG P, PAN TL, YUNG BY. Association of nucleophosmin/B23 mRNA expression with clinical outcome in patients with bladder carcinoma. *Urology* 2004; 64: 839–844. <https://doi.org/10.1016/j.urolgy.2004.05.020>
- [32] FALINI B, MECUCCI C, TIACCI E, ALCALAY M, ROSATI R et al. Cytoplasmic nucleophosmin in acute myelogenous leukemia with a normal karyotype. *N Engl J Med* 2005; 352: 254–266. <https://doi.org/10.1056/NEJMoa041974>
- [33] VASSILIOU GS, COOPER JL, RAD R, LI J, RICE S et al. Mutant nucleophosmin and cooperating pathways drive leukemia initiation and progression in mice. *Nat Genet* 2011; 43: 470–475. <https://doi.org/10.1038/ng.796>
- [34] BALUSU R, FISKUS W, RAO R, CHONG DG, NALLURI S et al. Targeting levels or oligomerization of nucleophosmin 1 induces differentiation and loss of survival of human AML cells with mutant NPM1. *Blood* 2011; 118: 3096–3106. <https://doi.org/10.1182/blood-2010-09-309674>
- [35] MEANI N, ALCALAY M. Role of nucleophosmin in acute myeloid leukemia. *Expert Rev Anticancer Ther* 2009; 9: 1283–1294. <https://doi.org/10.1586/era.09.84>
- [36] KAO HW, LIANG DC, WU JH, KUO MC, WANG PN et al. Gene mutation patterns in patients with minimally differentiated acute myeloid leukemia. *Neoplasia* 2014;16: 481–488. <https://doi.org/10.1016/j.neo.2014.06.002>
- [37] SUN JZ, LU Y, XU Y, LIU F, LI FQ et al. Epidermal growth factor receptor expression in acute myelogenous leukaemia is associated with clinical prognosis. *Hematol Oncol* 2012; 30: 89–97. <https://doi.org/10.1002/hon.1002>
- [38] BHATTACHARYYA J, NATH S, SAIKIA KK, SAXENA R, SAZAWAL S et al. Prevalence and Clinical Significance of FLT3 and NPM1 Mutations in Acute Myeloid Leukaemia Patients of Assam, India. *Indian J Hematol Blood Transfus* 2018; 34: 32–42. <https://doi.org/10.1007/s12288-017-0821-0>

[https://doi.org/10.4149/neo\\_2023\\_221021N1039](https://doi.org/10.4149/neo_2023_221021N1039)

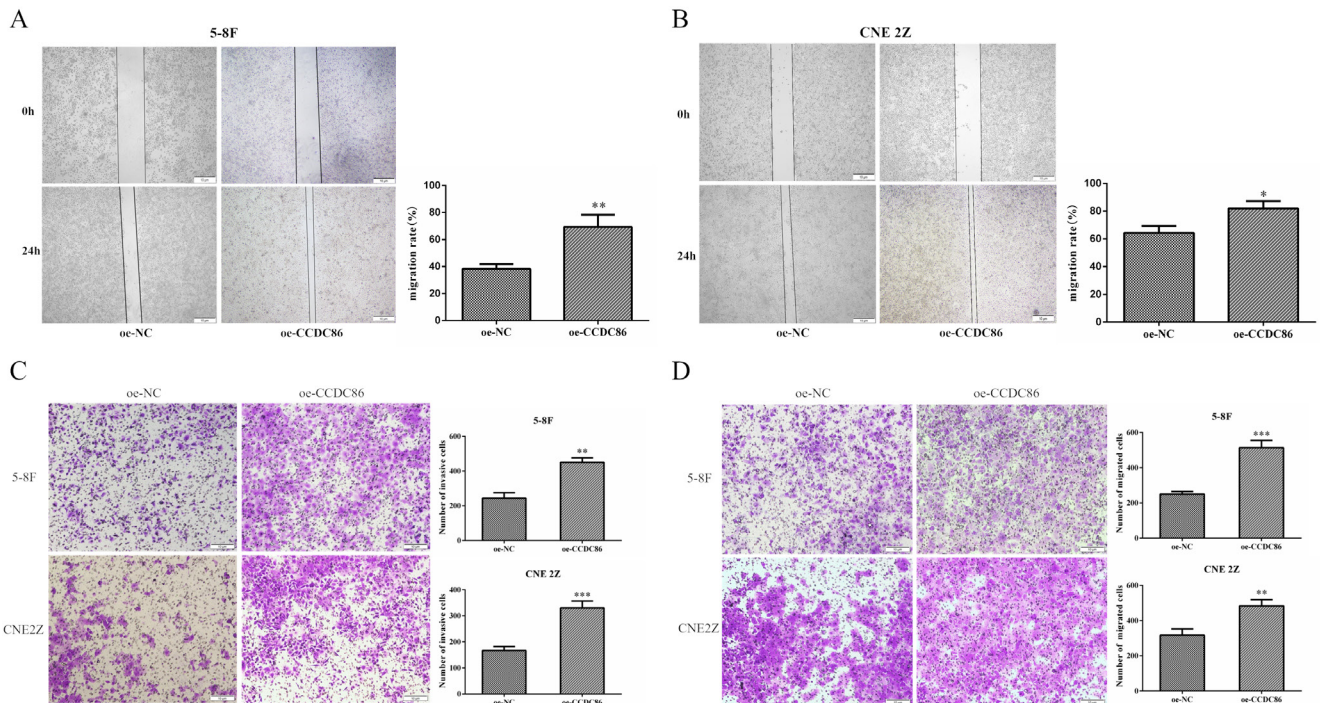
## CCDC86 promotes the aggressive behavior of nasopharyngeal carcinoma by positively regulating EGFR and activating the PI3K/Akt signaling

Zhi WANG<sup>1,†</sup>, Tao ZHOU<sup>2,†</sup>, Xubo CHEN<sup>1</sup>, Xinhua ZHU<sup>1</sup>, Bing LIAO<sup>1</sup>, Jianguo LIU<sup>1</sup>, Siqi LI<sup>1</sup>, Ting TAN<sup>1</sup>, Yuehui LIU<sup>1,\*</sup>

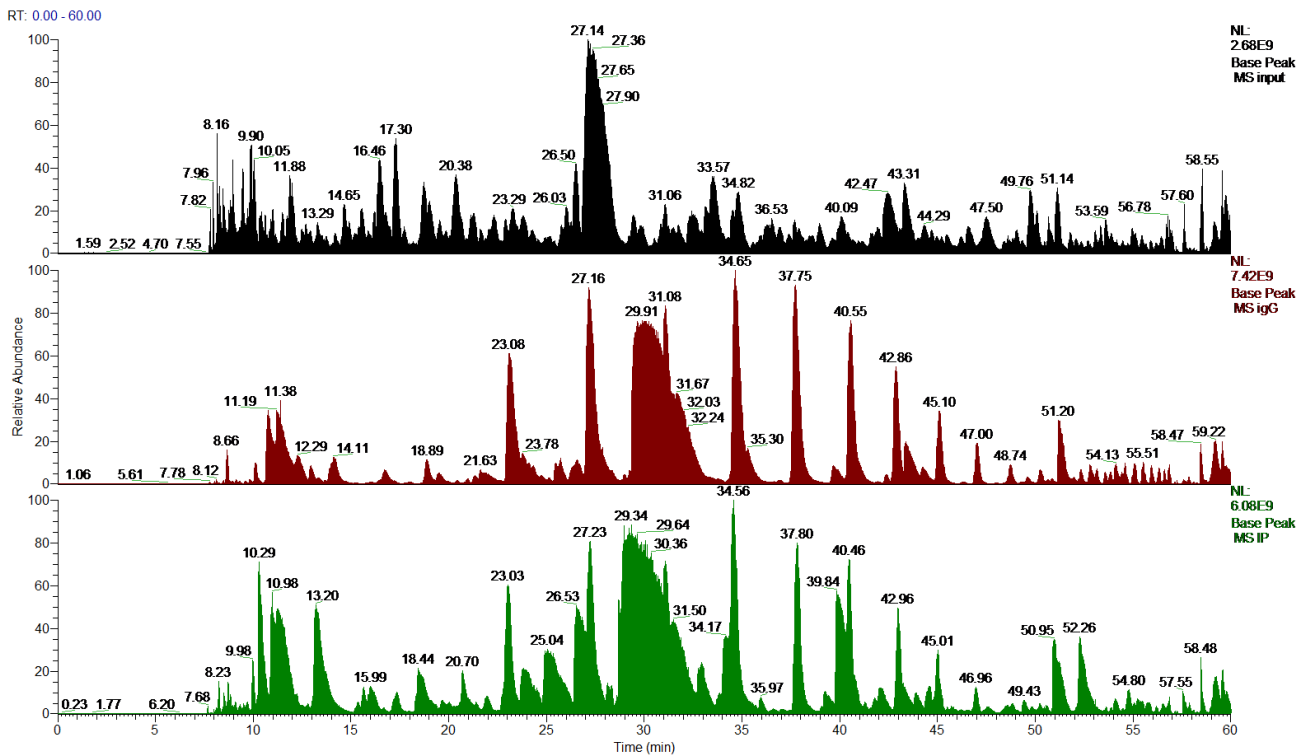
### Supplementary Information



Supplementary Figure S1. A) Cell migration of 5-8F and CNE2Z cells with stable CCDC86 knockdown was determined by wound-healing assays (magnification 100 $\times$ ). B, C) Migration and invasion of 5-8F and CNE2Z cells with stable CCDC86 knockdown was determined by Transwell migration and invasion assays (magnification 200 $\times$ ). The data are present as the mean $\pm$ SD of three independent experiments. \*\* $p$ <0.01, \*\*\* $p$ <0.001



Supplementary Figure S2. A, B) Migration of 5-8F and CNE2Z cells stably overexpressing CCDC86 was determined by wound-healing assays (magnification 100 $\times$ ). C, D) Migration and invasion of 5-8F and CNE2Z cells stably overexpressing CCDC86 was determined by Transwell migration and invasion assays (magnification 200 $\times$ ). The data are presented as the mean $\pm$ SD of three independent experiments. \* $p$ <0.05, \*\* $p$ <0.01, \*\*\* $p$ <0.001



Supplementary Figure S3. The base peak of mass spectra. Input, IgG and IP (from top to bottom) sample mass spectrum base peaks.

**Supplementary Table S1. Detailed information of the antibodies for WB used in this study.**

<b>Antibody name (the primary antibodies for WB)</b>	<b>Species</b>	<b>Company</b>	<b>Catalog No.</b>	<b>Dilution</b>	<b>Protein size</b>
CCDC86	Rabbit	Thermo Fisher	PA5-59617	1:1750	72 kDa
EGFR	Rabbit	Abcam	ab52894	1:1000	175 kDa
E-cadherin	Rabbit	Abcam	ab133597	1:1000	97 kDa
$\beta$ -catenin	Rabbit	Abcam	ab6302	1:4000	94 kDa
Vimentin	Mouse	Abcam	ab8978	1:200	57 kDa
MMP2	Rabbit	Abcam	ab97779	1:500	74 kDa
MMP9	Rabbit	Abcam	ab38898	1:1000	92 kDa
PI3K	Rabbit	Affinity	AF5121	1:1000	83 kDa
P-PI3K(Tyr607)	Rabbit	Affinity	AF3241	1: 1000	80 kDa
Akt	Rabbit	Affinity	AF6261	1: 1000	60 kDa
P-Akt (Ser473)	Rabbit	Affinity	AF0016	1:1000	60 kDa
GAPDH	Rabbit	Abcam	ab181602	1: 10000	36 kDa

<b>Antibody name (the secondary antibodies for WB)</b>	<b>Company</b>	<b>Catalog No.</b>	<b>Dilution</b>
Goat anti-Rabbit IgG (H+L) Secondary Antibody, HRP	Thermo Fisher	65-6120	1: 5000
Goat anti-Mouse IgG (H+L) Secondary Antibody, HRP	Thermo Fisher	31430	1: 5000

**Supplementary Table S2. Detailed information of the antibodies for Co-IP used in this study.**

<b>Antibody name (the primary antibodies for Co-IP)</b>	<b>Species</b>	<b>Company</b>	<b>Catalog No.</b>	<b>Dilution</b>	<b>Protein size</b>
CCDC86	Rabbit	Thermo Fisher	PA5-59617	1:1750	72 kDa
NPM1	Rabbit	Abcam	ab52644	1: 200000	33 kDa

<b>Antibody name (the secondary antibodies Co-IP)</b>	<b>Company</b>	<b>Catalog No.</b>	<b>Dilution</b>
Goat anti-Rabbit IgG (H+L) Secondary Antibody, HRP	Thermo Fisher	65-6120	1: 5000